

When Robustness Meets Conservativeness: Conformalized Uncertainty Calibration for Balanced Decision Making

Wenbin Zhou
Carnegie Mellon University

Shixiang Zhu
Carnegie Mellon University

Abstract

Robust optimization safeguards decisions against uncertainty by optimizing against worst-case scenarios, yet their effectiveness hinges on a prespecified robustness level that is often chosen ad hoc, leading to either insufficient protection or overly conservative and costly solutions. Recent approaches using conformal prediction construct data-driven uncertainty sets with finite-sample coverage guarantees, but they still fix coverage targets a priori and offer little guidance for selecting robustness levels. We propose a new framework that provides distribution-free, finite-sample guarantees on both miscoverage and regret for any family of robust predict-then-optimize policies. Our method constructs valid estimators that trace out the miscoverage-regret Pareto frontier, enabling decision-makers to reliably evaluate and calibrate robustness levels according to their cost-risk preferences. The framework is simple to implement, broadly applicable across classical optimization formulations, and achieves sharper finite-sample performance than existing approaches. These results offer the first principled data-driven methodology for guiding robustness selection and empower practitioners to balance robustness and conservativeness in high-stakes decision-making.

1 Introduction

Decision-making under uncertainty is a fundamental challenge in operations research, machine learning, and economics. From utilities preparing for extreme weather [Chen et al., 2025] to financial institutions managing investment risk [Fabozzi et al., 2007], decision-makers must act without knowing the exact outcomes of their choices. Robust optimization (RO) has emerged as a leading paradigm for addressing

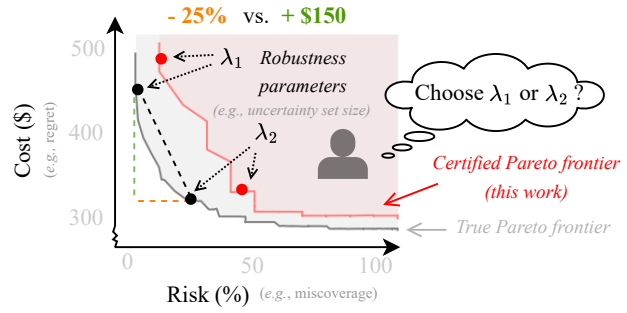


Figure 1: A stylized example illustrating the use of our proposed framework. Instead of heuristically fixing a risk level (e.g., 5%), the decision-maker can use this frontier to select a preferred trade-off. For instance, the curve indicates that reducing risk by up to 25% (orange dashed line) yields a cost reduction of at least \$150, corresponding to roughly a 30% improvement (green dashed line).

this challenge: rather than optimizing for the most likely outcome, RO seeks decisions that remain effective under the worst-case realization within a pre-specified uncertainty set [Beyer and Sendhoff, 2007]. For instance, grid operators may schedule generator dispatch robust to worst-case demand fluctuations [Bertsimas et al., 2012], while portfolio managers may hedge against worst-case returns consistent with historical data [Goldfarb and Iyengar, 2003].

A standard way to operationalize the RO problems is through the predict-then-optimize (PTO) framework [Bertsimas and Kallus, 2020]: a predictive model first suggests an uncertainty set for the outcome, and the decision-maker then chooses a decision that minimizes the worst-case loss within that set. In traditional RO, this uncertainty set is pre-specified, often as a polyhedral or ellipsoidal region around forecasts [Gabrel et al., 2014]. Its size is governed by a robustness parameter, typically selected through heuristics. For instance, setting the radius to a multiple of the forecast variance. More recently, conformal

prediction (CP) has emerged as a data-driven alternative for defining uncertainty sets, providing finite-sample coverage guarantees that the realized outcome lies within the set with a prescribed probability [Vovk et al., 2005]. This approach has also been incorporated into robust optimization, where CP-based sets define the uncertainty region used for decision-making [Patel et al., 2024b].

While these approaches have expanded the scope and rigor of robust decision-making, they leave a critical question unresolved: *how should one choose the robustness level?* In RO, the radius of the uncertainty set—or in CP, the confidence level—directly governs the trade-off between protection and efficiency. In practice, this choice is typically made heuristically: by fixing conventional confidence levels (e.g., 95%) or by tuning against historical simulations [Lam and Zhou, 2017]. Such methods provide little theoretical guidance, and when data are scarce, simulation-based estimates can be unreliable. This gap makes it difficult for practitioners to balance safety with performance, and decisions are often more conservative than necessary.

In this paper, we propose a new statistical framework that enables decision-makers to evaluate and select robustness levels with explicit trade-offs. Our method is inspired by conformal risk control (CRC) [Angelopoulos et al., 2022], but inverts its logic. Standard CRC begins by prescribing a target risk level and adaptively constructs a set or decision rule to satisfy that risk constraint. By contrast, our inverse CRC framework takes an uncertainty set as given, and then certifies the actual risk level it incurs. This inversion is crucial: it allows us to quantify both miscoverage (the probability that the outcome falls outside the set) and regret (the expected cost relative to an oracle) across all risk levels with rigorous guarantees. Practically, this enables decision-makers to explore the trade-off between robustness and conservativeness in a reliable manner. For example, in the stylized setting of Figure 1, our method may show that reducing coverage by up to 25% can yield a cost reduction of at least \$150. Such insights enable decision-makers to adjust robustness levels adaptively, achieving more cost-effective solutions rather than relying on ad hoc or overly conservative heuristics.

The approach is also straightforward to implement: given calibration data, we construct valid estimators for miscoverage and regret across all robustness levels and use them to trace out a Pareto frontier of risk trade-offs under a mild condition. Theoretical results show that these estimators are reliable, enjoy sharp finite-sample guarantees, and apply broadly to various robust optimization problems. Our numer-

ical results demonstrate that the estimator successfully traces Pareto frontiers that are both valid and tight, and can also effectively guide decision-makers toward robustness parameters that are near-optimal for achieving the desired miscoverage-regret tradeoff.

The contributions of this paper are threefold:

1. We propose a principled framework for “inverse” conformal risk control, enabling risk quantification with respect to any arbitrary loss function.
2. We develop a distribution-free estimator of both miscoverage and regret across robustness levels in robust optimization. Our approach is computationally efficient, valid in finite samples, and establishes the first certified Pareto frontier for robust optimization under mild assumptions.
3. We illustrate the broad applicability of our approach on classical optimization problems, demonstrating how it enables decision-makers to reliably calibrate robustness by balancing robustness against conservativeness.

Related Work Our work builds on the broad literature on PTO problems, where a decision-maker observes covariates and must act before outcomes are realized [Bertsimas and Kallus, 2020]. The PTO paradigm has been studied both in two-stage approaches, where one first learns a predictive model and then optimizes with respect to the prediction, and in decision-focused methods that train predictors end-to-end with the downstream objective in mind [Mandi et al., 2024]. Our work complements both streams: instead of introducing new predictors or losses, we develop finite-sample guarantees for evaluating the risk of any robust PTO policy family, enabling practitioners to quantify robustness–conservativeness trade-offs without altering their learning pipeline.

Within PTO, robust optimization (RO) and distributionally robust optimization (DRO) are widely used to hedge against uncertainty. RO approaches define a deterministic uncertainty set and minimize worst-case cost [Ben-Tal and Nemirovski, 2002, Beyer and Sendhoff, 2007, Gabrel et al., 2014], while DRO places ambiguity sets around distributions, typically ϕ -divergence or Wasserstein balls, and exploits convex duality to reformulate the robust problem [Rahimian and Mehrotra, 2019, Lin et al., 2022]. These methods yield increasingly conservative selectors as the robustness parameter grows. Our framework is orthogonal: given any nested family of uncertainty sets, whether from RO or DRO, we provide distribution-free bounds on realized risks.

A related line of research leverages conformal prediction (CP) to construct uncertainty sets for robust optimization [Patel et al., 2024a, Patel et al., 2024b, Chen et al., 2025]. Here, CP provides data-driven prediction set with finite-sample marginal coverage guarantees [Papadopoulos et al., 2002, Vovk et al., 2005, Zhang et al., 2025], and the robust decision is optimized against these sets. While effective, this approach prescribes the coverage target *a priori* and tunes the set to achieve it [Patel et al., 2024b]. In contrast, our method inverts the perspective: we take prediction set as given—whether from CP, RO, or DRO—and quantify the actual risks it incurs [Gauthier et al., 2025a, Zhou et al., 2025]. This inversion avoids adaptivity penalties, provides simultaneous guarantees for miscoverage and regret, and ties the risk trade-off curve to the Pareto frontier under majorant consistency.

Our framework is related to the multi-objective optimization literature [Marler and Arora, 2004, Gunantara, 2018], as both aim to characterize the Pareto frontier that formalizes trade-offs among competing goals. The key distinction is that we avoid the nested structure often required in multi-objective formulations: instead of embedding one optimization problem (*e.g.*, robust optimization) inside another (*e.g.*, regret minimization), we exploit the simple structure of the miscoverage–regret trade-off. By directly enumerating over robustness parameters and certifying risk trade-offs from calibration data via conformal techniques, our approach yields a lightweight procedure that admits explicit finite-sample guarantees—something generally unattainable with multi-objective optimization frameworks.

Finally, our work is related to conformal risk control (CRC) [Angelopoulos et al., 2022] and its extensions such as [Farinhias et al., 2023, Teneggi et al., 2023]. Standard CRC prescribes a risk target and ensures validity, while backward or inverse conformal methods start from candidate sets and estimate their realized risk, sometimes via e-values [Balinsky and Balinsky, 2024, Gauthier et al., 2025b]. We differ in three ways: (*i*) we analyze fixed *a priori* robustness levels, allowing tighter analytic bounds; (*ii*) we extend beyond coverage to regret of a robust decision relative to the oracle; and (*iii*) our estimator attains validity with sharper finite-sample error rates than other methods. In this way, our work unifies PTO, RO, and CP, but with a new emphasis on jointly certifying robustness and conservativeness along the Pareto frontier.

2 Problem Setup

We consider a general decision-making problem under uncertainty [Bertsimas and Kallus, 2020]. A decision-maker observes a contextual feature vector $X \in \mathcal{X}$ and must choose a decision variable $z \in \mathcal{Z}$ before the outcome $Y \in \mathcal{Y}$ is realized. The pair (X, Y) is drawn from an underlying distribution \mathcal{P} . The quality of a decision z in the presence of outcome y is measured by a cost function $f : \mathcal{Y} \times \mathcal{Z} \rightarrow \mathbb{R}$.

To account for uncertainty from the unknown joint distribution \mathcal{P} , a standard approach is to introduce an *uncertainty set* that safeguards against plausible realizations of Y . Specifically, we introduce a family of context-dependent uncertainty sets:

$$\left\{ \mathcal{C}_\lambda(X) \subseteq \mathcal{Y} : \lambda \in \Lambda \subseteq \mathbb{R}_+ \right\},$$

indexed by a robustness parameter λ , with the convention that larger λ yields larger sets: $\lambda_1 \leq \lambda_2 \Rightarrow \mathcal{C}_{\lambda_1}(X) \subseteq \mathcal{C}_{\lambda_2}(X)$ for all X . For instance, one may construct $\mathcal{C}_\lambda(X)$ as an euclidean ball centered at the conditional mean $\hat{g}(X) \approx \mathbb{E}[Y|X]$, where \hat{g} is estimated from data, and take λ as the radius of the ball. Given X , the robust decision is obtained by solving:

$$z_\lambda^*(X) := \arg \min_{z \in \mathcal{Z}} \max_{y \in \mathcal{C}_\lambda(X)} f(y, z). \quad (1)$$

A key challenge is to select λ so that the robust decision strikes the right balance between *regret* and *miscoverage* as illustrated by Figure 2: If the uncertainty set $\mathcal{C}_\lambda(X)$ is too small, the decision may fail to provide sufficient protection against adverse outcomes; If the set is too large, the solution to (1) may be overly conservative and incur an undesirably large regret. We assess each λ using two performance metrics given a pair of (X, Y) :

$$\begin{aligned} I_\lambda(X, Y) &:= \mathbb{1}[Y \notin \mathcal{C}_\lambda(X)], \\ R_\lambda(X, Y) &:= f(Y, z_\lambda^*(X)) - \min_{z \in \mathcal{Z}} f(Y, z). \end{aligned}$$

Specifically, for a given pair (X, Y) , $I_\lambda \in \{0, 1\}$ indicates whether the realized outcome Y is excluded from the uncertainty set $\mathcal{C}_\lambda(X)$, and R_λ measures the performance gap of adopting robust decision $z_\lambda^*(X)$ relative to the oracle decision under the realized Y .

The objective of this study is to answer two fundamental questions: For any prescribed robustness level λ , *how robust does it protect against unknown outcomes?* and *how costly is this protection in terms of conservativeness?* Formally, we seek to construct estimators $\hat{\alpha}_I(\lambda)$ and $\hat{\alpha}_R(\lambda)$ that can be trusted to provide reliable assessments for any prespecified $\lambda \in \Lambda$:

$$\hat{\alpha}_I(\lambda) \geq \mathbb{E}[I_\lambda(X, Y)] = 1 - \mathbb{P}[Y \in \mathcal{C}_\lambda(X)], \quad (2)$$

$$\hat{\alpha}_R(\lambda) \geq \mathbb{E}[R_\lambda(X, Y)]. \quad (3)$$

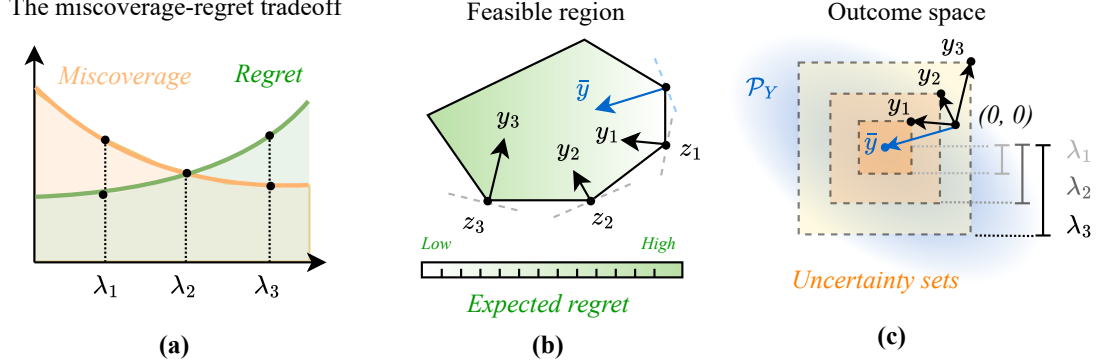


Figure 2: Illustration of the problem setup with a simple robust linear optimization problem. Panel (a) shows the miscoverage-regret tradeoff across three robustness parameters ($\lambda_1, \lambda_2, \lambda_3$). Panel (b) depicts the corresponding robust decisions (z_1, z_2, z_3), which differ from the expected optimal decision z^* . Panel (c) illustrates an ℓ_∞ -ball uncertainty set \mathcal{C}_λ for the outcome variable Y , with the three adversarial outcome vectors (y_1, y_2, y_3) labeled. The robustness parameters correspond to the radii of these ℓ_∞ -norm sets.

Estimating these two upper bounds traces out the certified Pareto frontier that trades off between regret and miscoverage in the worst-case scenario, revealing how reducing miscoverage typically increases regret, and vice versa. By examining $\hat{\alpha}_I(\lambda)$ and $\hat{\alpha}_R(\lambda)$ across candidate λ , practitioners can select the point that best balances protection against conservativeness in line with their risk tolerance.

3 Methodology

This section first introduces a general statistical framework for “inverse” conformal risk control motivated by [Angelopoulos et al., 2022, Patel et al., 2024b], designed to estimate an upper bound on risk defined with respect to an arbitrary loss function. We then demonstrate how this framework can be applied to estimate both miscoverage rate (2) and regret (3) of a robust solution to problem (1). Finally, we show that these estimates are reliable and valid, *i.e.*, the expected upper bound is guaranteed to hold, and that they directly characterize the certified Pareto frontier as the robustness level λ varies.

3.1 Proposed Algorithm

Let $\ell_\lambda : \mathcal{X} \times \mathcal{Y} \rightarrow \mathbb{R}$ be a family of nonnegative loss (*e.g.*, miscoverage or regret), where ℓ_λ is monotone in λ according to the definition of \mathcal{C}_λ . We assume access to a calibration dataset of n paired samples, denoted as $\mathcal{D} = \{(X_i, Y_i)\}_{i=1}^n$. Given a test data pair (X_{n+1}, Y_{n+1}) , our goal is to construct an estimator, denoted $\hat{\alpha}_\ell(\lambda)$, from the calibration data \mathcal{D} such that

$$\hat{\alpha}_\ell(\lambda) \geq \mathbb{E} [\ell_\lambda(X_{n+1}, Y_{n+1})]. \quad (4)$$

This objective subsumes both (2) and (3), and can be interpreted as an “inverse” form of the conformal risk control (CRC) [Angelopoulos et al., 2022]. Specifically, CRC begins by prescribing a desired risk level α on the expected loss and then finds λ that guarantees:

$$\mathbb{E} [\ell_\lambda(X_{n+1}, Y_{n+1})] \leq \alpha.$$

By contrast, our framework reverses this perspective. Instead of taking a target risk level α as given, we take the uncertainty set—indexed by robustness level λ —as fixed, and then ask: *what is the actual risk level guaranteed by this choice?*

Before describing our proposed algorithm, we first state two assumptions that is considered. First, we assume the exchangeability between this dataset with the test data pair.

Assumption 1. *The calibration data \mathcal{D} and the test point (X_{n+1}, Y_{n+1}) are drawn exchangeably from distribution \mathcal{P} .*

This assumption is standard in the conformal prediction literature [Vovk et al., 2005] and subsumes many common settings, including the case of *i.i.d.* sampling. Furthermore, we assume that there exists a known uniform upper bound on the regret.

Assumption 2. *There exists a known constant $B \geq 0$ such that for all $\lambda \in \Lambda$, $\mathbb{P}\{0 \leq \ell_\lambda(X, Y) \leq B\} = 1$.*

Assumption 2 typically requires some prior knowledge of the loss function to verify. In many cases, however, the bound B is straightforward to obtain—for example, when the loss function is inherently bounded or when the distribution \mathcal{P} has bounded support.

Given the two assumptions above, we propose a conformalized risk estimator as follows:

Algorithm 1 CREME: Conformal REgret-Miscoverage Estimate

Require: Calibration data $\mathcal{D} := \{(x_i, y_i)\}_{i=1}^n$; robustness parameter set $\{\lambda_i\} \subseteq \Lambda$;

- 1: $\hat{\mathcal{F}} \leftarrow \emptyset$ initialize Pareto frontier;
- 2: **for** $\lambda \in \{\lambda_i\}$ **do**
- 3: $\bar{I}_n(\lambda) \leftarrow \sum_{i=1}^n I_\lambda(x_i, y_i)/n$;
- 4: $\bar{R}_n(\lambda) \leftarrow \sum_{i=1}^n R_\lambda(x_i, y_i)/n$;
- 5: $\tilde{\alpha}_R(\lambda) \leftarrow$ compute (6) with $\bar{R}_n(\lambda)$, $B = R_{\max}$;
- 6: $\tilde{\alpha}_I(\lambda) \leftarrow$ compute (6) with $\bar{I}_n(\lambda)$, $B = 1$;
- 7: $\hat{\mathcal{F}} \leftarrow \hat{\mathcal{F}} \cup \{(\tilde{\alpha}_I(\lambda), \tilde{\alpha}_R(\lambda))\}$;
- 8: **end for**
- 9: Remove dominated points from $\hat{\mathcal{F}}$ (keep only tuples not weakly worse in both coordinates);
- 10: **return** Certified Pareto frontier $\hat{\mathcal{F}}$.

Proposition 1. Let $\bar{\ell}_n(\lambda)$ denote the average calibration loss, i.e., $\bar{\ell}_n(\lambda) := \frac{1}{n} \sum_{i=1}^n \ell_\lambda(x_i, y_i)$. The proposed risk estimator is defined as

$$\hat{\alpha}_\ell(\lambda) = \inf \left\{ \alpha \in (0, B) : B - \bar{\ell}_n(\lambda) \geq \frac{\lceil (n+1)(B-\alpha) \rceil}{n} \right\}, \quad (5)$$

In practice, a more convenient approximation is

$$\tilde{\alpha}_\ell(\lambda) = \frac{n}{n+1} \bar{\ell}_n(\lambda) + \frac{B}{n+1}, \quad (6)$$

which can be derived by relaxing the ceiling operator in (5). This form requires only the empirical average calibration loss $\bar{\ell}_n(\lambda)$ plus an adjustment $B/(n+1)$ that accounts for the worst-case contribution of the unseen test point, guaranteed to lie in $[0, B]$ by Assumption 2. This conservative correction is crucial for ensuring validity: without it, the empirical estimate alone would not guarantee coverage on new data. The complexity of computing $\bar{\ell}_n(\lambda)$ is linear in the number of calibration samples, and the adjustment is constant, making $\hat{\alpha}(\lambda)$ efficient to evaluate for each candidate λ .

Finally, we construct the miscoverage-regret frontier using the above estimator as follows: For each candidate robustness level λ , we first solve the robust problem in (1) to obtain the decision rule $z_\lambda^*(\cdot)$, then evaluate the induced miscoverage and regret losses on calibration data. These empirical averages are corrected using the conservative adjustment in Proposition 1 to yield valid upper-bound estimates of risk. Collecting the pairs $(\hat{\alpha}_I(\lambda), \hat{\alpha}_R(\lambda))$ across all λ forms the empirical frontier, which is then Pareto-pruned to remove dominated points. The pseudocode in Algorithm 1 summarizes the entire proposed method.

3.2 Theoretical Analysis

We establish two key theoretical properties of the proposed estimator. First, we prove its validity, showing that under the exchangeability assumption, the proposed estimator $\hat{\alpha}_\ell(\lambda)$ upper bounds the true risk for any specification of the robustness parameter λ . Then, we demonstrate that under a majorant consistency assumption, the conservative trajectory traced by the estimator $(\hat{\alpha}_I(\lambda), \hat{\alpha}_R(\lambda))$ by varying λ characterizes a certified Pareto frontier.

Theorem 1 (Validity). *Under Assumption 1 and 2, the estimator $\hat{\alpha}_\ell(\lambda)$ in (5) satisfies*

$$\mathbb{E}[\hat{\alpha}_\ell(\lambda)] \geq \mathbb{E}[\ell_\lambda(X_{n+1}, Y_{n+1})].$$

Proof of Theorem 1. We prove by showing:

$$\mathbb{E}[\hat{\alpha}_\ell(\lambda)] \stackrel{(a)}{\geq} \mathbb{E}[\tilde{\alpha}_\ell(\lambda)] \stackrel{(b)}{\geq} \mathbb{E}[\ell_\lambda(X_{n+1}, Y_{n+1})].$$

To prove (a), notice that $\tilde{\alpha}_\ell(\lambda)$ is equivalent to (5) after removing the ceiling operator, and by

$$\frac{(n+1)(B - \hat{\alpha}_\ell(\lambda))}{n} \leq \frac{\lceil (n+1)(B - \hat{\alpha}_\ell(\lambda)) \rceil}{n} \stackrel{(5)}{\leq} B - \bar{\ell}_n(\lambda),$$

therefore $\hat{\alpha}_\ell(\lambda) \geq \tilde{\alpha}_\ell(\lambda)$ almost surely, which implies (a). To prove (b), we expand the difference of two sides of (b) by using the definition of $\tilde{\alpha}_\ell(\lambda)$ in (6):

$$\begin{aligned} & \mathbb{E}[\tilde{\alpha}_\ell(\lambda)] - \mathbb{E}[\ell_\lambda(X_{n+1}, Y_{n+1})] \\ &= \left(\frac{n}{n+1} - 1 \right) \mathbb{E}[\ell_\lambda(X_{n+1}, Y_{n+1})] + \frac{B}{n+1} \\ &= \frac{B - \mathbb{E}[\ell_\lambda(X_{n+1}, Y_{n+1})]}{n+1} \geq 0. \end{aligned}$$

where the first equation follows from Assumption 1, and the inequality follows from Assumption 2. This proves (b) holds and thus concludes the proof. \square

We note that our notion of validity resembles the idea of post-hoc validity studied in the literature, such as [Gauthier et al., 2025a]. In both cases, the prediction sets are specified first, and the analysis then determines the corresponding risk guarantee α . However, there is a key difference: In prior work, the candidate set is typically data-dependent, and validity is ensured through post-hoc adjustment, often relying on e-value methods [Balinsky and Balinsky, 2024, Gauthier et al., 2025a, Gauthier et al., 2025b]. By contrast, in our framework the robustness level λ —and hence the uncertainty set \mathcal{C}_λ —is specified *a priori*, independent of the data. The estimator $\hat{\alpha}_\ell(\lambda)$ then directly provides a guaranteed bound on the associated risk without adaptive tuning. As a result, our method preserves validity with substantially higher accuracy,

i.e., a smaller deviation from the true risk, compared to e-value-based approaches.

Additionally, under a slightly more demanding *i.i.d.* conditioning, we can also establish a finite-sample error bound for the proposed estimator.

Proposition 2 (Finite-sample error bound). *Under Assumption 2 and suppose $\{(x_i, y_i)\}_{i=1}^{n+1}$ are i.i.d. sampled, then for any $\delta > 0$ and $\lambda \in \Lambda$, with probability at least $1 - \delta$,*

$$\begin{aligned} & |\hat{\alpha}(\lambda) - \mathbb{E}[\ell_\lambda(X_{n+1}, Y_{n+1})]| \\ & \leq \frac{B}{n+1} \left(\sqrt{\frac{n}{2} \log \left(\frac{2}{\delta} \right)} + 2 + \frac{1}{B} \right) =: \epsilon \end{aligned} \quad (7)$$

Proposition 2 is useful, as when combined with Theorem 1, we can now a valid *one-shot* estimator with at least probability $1 - \delta$ by offsetting it with the error defined in (7):

$$\mathbb{P}\{\hat{\alpha}(\lambda) + \epsilon \geq \mathbb{E}[\ell(X_{n+1}, Y_{n+1})]\} \geq 1 - \delta.$$

Since this error bound decays to zero at an $O(n^{-1/2})$ parametric rate, this means that the estimator is sample efficient and asymptotically consistent.

Next, we show that the trajectory describing the miscoverage-regret trade-off is (weakly) decreasing under the standard *majorant consistency* assumption [Delage and Ye, 2010, Rahimian and Mehrotra, 2019, Mohajerin Esfahani and Kuhn, 2018]. This assumption is crucial for guaranteeing that the trade-off curve preserves a monotone structure, thereby ensuring the existence of a well-defined Pareto frontier.

Assumption 3 (Majorant consistency). *For each robustness level λ and context x , let $z_\lambda^*(x)$ be a measurable robust selector. For all $\lambda_1 \leq \lambda_2$, there is*

$$\mathbb{E}[f(Y, z_{\lambda_1}^*(X))|X] \leq \mathbb{E}[f(Y, z_{\lambda_2}^*(X))|X] \text{ a.s.} \quad (8)$$

Assumption 3 describes the condition that shrinking the uncertainty set does not increase the conditional expected realized cost. It holds in a broad range of standard optimization problems, including robust linear optimization with polyhedral or ellipsoidal uncertainty sets [Ben-Tal and Nemirovski, 1999], robust quadratic optimization, regression with convex loss functions (e.g., squared, absolute, or Huber loss) under norm-ball uncertainty [Ben-Tal and Nemirovski, 2001], and robust classification with convex surrogate losses (e.g., hinge or logistic) [Bertsimas et al., 2011]. It is also directly implied by distributionally robust optimization (DRO) formulations with Wasserstein or ϕ -divergence balls, where monotonicity of the robust objective in the size of the ball is well established

[Delage and Ye, 2010, Rahimian and Mehrotra, 2019, Mohajerin Esfahani and Kuhn, 2018]. We present an example and a counterexample for Assumption 3 in Appendix A.

Combined with the properties of nested uncertainty sets and bounded regret in our problem setting, we can prove that the image of the trade-off curve coincides with the Pareto frontier of the robust policy family. The proof can be found in Appendix C.

Proposition 3 (True Pareto frontier). *Let $\alpha_I(\lambda) := \mathbb{E}[I_\lambda(X, Y)]$ and $\alpha_R(\lambda) := \mathbb{E}[R_\lambda(X, Y)]$. Under Assumption 3, for any $\lambda_1 \leq \lambda_2$,*

$$\alpha_I(\lambda_1) \geq \alpha_I(\lambda_2), \quad \alpha_R(\lambda_1) \leq \alpha_R(\lambda_2).$$

Hence, the parametric curve $\lambda \mapsto (\alpha_I(\lambda), \alpha_R(\lambda))$ is (weakly) decreasing. Its image is the Pareto frontier within the policy family $\{z_\lambda^ : \lambda \in \Lambda\}$.*

Corollary 1 (Certified Pareto Frontier). *Given that estimators $\hat{\alpha}_I(\lambda), \hat{\alpha}_R(\lambda)$ satisfy*

$$\hat{\alpha}_I(\lambda) \geq \alpha_I(\lambda), \quad \hat{\alpha}_R(\lambda) \geq \alpha_R(\lambda), \quad \forall \lambda \in \Lambda.$$

Then the set $\widehat{\mathcal{F}} := \{(\hat{\alpha}_I(\lambda), \hat{\alpha}_R(\lambda)) : \lambda \in \Lambda\}$ forms a conservative outer approximation of the true risk set.

By Corollary 1, the lower-left envelope of $\widehat{\mathcal{F}}$ traces the certified Pareto frontier, thus providing guaranteed trade-offs between regret and miscoverage.

4 Experiments

This section evaluates the performance of our proposed algorithm in Algorithm 1, termed Conformal REgret MIScoverage Estimate (**CREME**). We focus on four representative optimization paradigms: (i) linear programming; (ii) the newsvendor problem (single-item inventory); (iii) portfolio optimization (long-only, mean-CVaR proxy); and (iv) the shortest path problem (equivalently, a unit flow problem). These problems are chosen because they exemplify widely studied optimization settings, and their regret can be efficiently computed using convex solvers. In each case, we designate certain parameters in the optimization objective (e.g., the cost vector) as the uncertain random variable Y , and the uncertainty set is defined as a ℓ_∞ ball centered at $\mathbb{E}[Y]$. Additional information for experimental configurations and omitted details in the remaining subsections are all deferred Section D.

4.1 Validity-Accuracy Analysis

We first evaluate the quality of the miscoverage-regret frontier produced by **CREME** using two metrics: *validity* and *accuracy*. Validity [Lei et al., 2018] measures

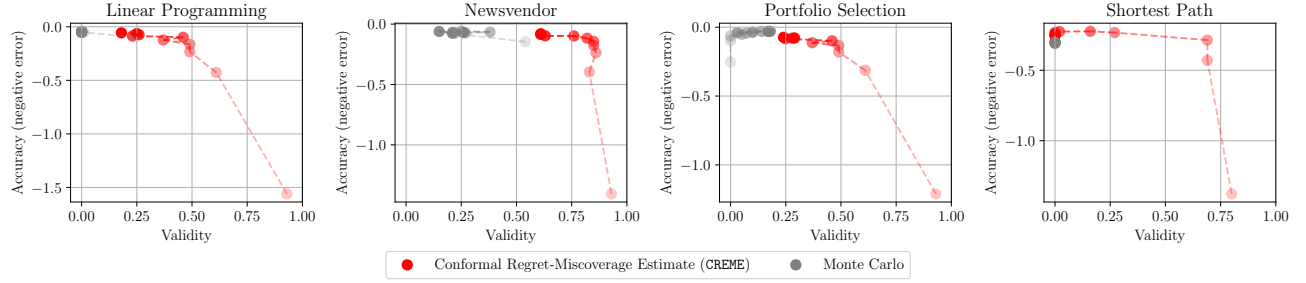


Figure 3: Validity-accuracy tradeoff curves under four optimization settings. Connected dots trace estimator performance as the number of calibration samples n increases from 1 to 50, with greater opacity indicating smaller n . The proposed method is shown in red, and the baseline Monte Carlo estimator in gray. Both axes represent metrics where higher values indicate better performance (\uparrow), so methods appearing closer to the upper-right corner are more desirable.

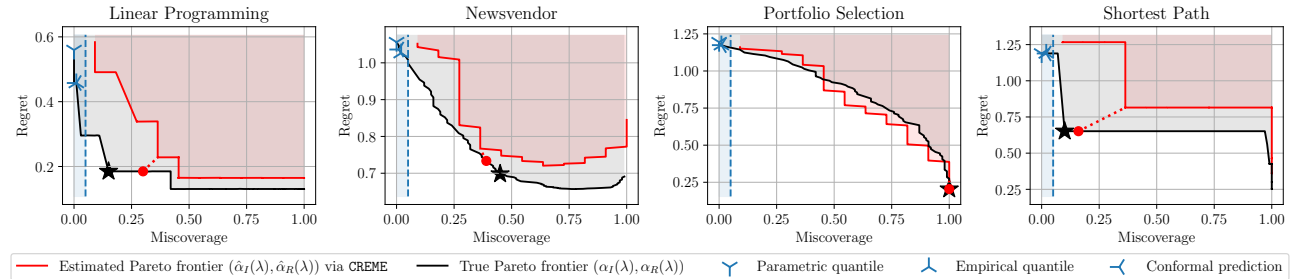


Figure 4: Miscoverage-regret tradeoff Pareto frontiers with attained solutions from each model. For a prespecified preference weighting, the black star denotes the true optimal tradeoff. The red dot indicates the tradeoff obtained from the estimated $\hat{\lambda}$ using CREME. Blue markers correspond to three baseline methods that identify λ values ensuring the miscoverage rate remains below 5% (vertical dashed blue line).

whether the estimator successfully upper bounds the true risk, while accuracy assesses the tightness of this bound. Formally, validity is defined as the proportion of trials in which both $\hat{\alpha}_R(\lambda)$ and $\hat{\alpha}_I(\lambda)$ satisfy their validity conditions. Accuracy [Zhou et al., 2025] is defined as the negative average Euclidean distance between the estimated front $(\hat{\alpha}_I(\lambda), \hat{\alpha}_R(\lambda))$ and the corresponding ground-truth front $(\alpha_I(\lambda), \alpha_R(\lambda))$, *i.e.*, negative of the mean error. When calculating these metrics, the ground truth front is approximated via Monte Carlo sampling of size 100 from the true distribution and averaged over 20 independent trials. Throughout our evaluation, λ is varied from zero to the support radius of Y .

Figure 3 presents the evaluation results, comparing CREME with the empirical Monte Carlo estimator (*i.e.*, $\bar{\ell}_n(\lambda)$). It can be seen that across all optimization settings, the Monte Carlo estimator (gray) tends to lie toward the left of the plot, while CREME (red) concentrates in the upper-right region. This difference arises because naive baselines are primarily designed for consistent estimation, achieving high accuracy without validity guarantees. In contrast, our proposed procedure strikes a balanced trade-off, maintaining strong per-

formance on both validity and accuracy, and tracing a Pareto frontier¹ over these two dimensions. These results not only support our theoretical analysis but also highlight that CREME is particularly well-suited for high-stakes decision-making tasks where both accuracy and validity are critical.

In particular, Figure 3 also provides deeper insights into the properties of CREME associated with the number of calibration data, which is shown in its performance trajectory (red dashed line). In the small-sample regime where there is limited calibration data, CREME exhibits relatively low accuracy but high validity, positioning itself in the lower-right region of the plot. This behavior is desirable: under uncertainty and limited resources, CREME prioritizes conservatism by erring on the side of validity. As the calibration sample size increases, the trajectory rises sharply along the accuracy axis (at an almost exponential rate) while declining only gradually along the validity axis (at an approximately linear rate). This imbalance in rates is crucial: it ensures the existence of a Pareto frontier and enables CREME to maintain fa-

¹This should be distinguished from the miscoverage-regret Pareto frontier in this paper.

vable trade-offs between validity and accuracy. In the large-sample regime, the trajectory converges toward the region occupied by the Monte Carlo estimator. This is expected, as our method is by design asymptotically consistent with the Monte Carlo estimator, explaining both the gradual deterioration of validity and the simultaneous improvement in accuracy as calibration size increases. Together, these observations provide a clear view into the internal behavior of CREME, demonstrating how it adapts across regimes and achieves strong trade-offs between accuracy and validity.

4.2 Decision Quality Evaluation

We also assess the quality of the robustness parameter $\hat{\lambda}$ selected by CREME. We show that given any pre-specified weight that encodes the decision-maker’s preference for the miscoverage–regret tradeoff, CREME can identify $\hat{\lambda}$ that closely approximates the optimal λ^* , thereby achieving tradeoff $(\hat{\alpha}_I(\hat{\lambda}), \hat{\alpha}_R(\hat{\lambda}))$ that approximates the optimal tradeoff $(\hat{\alpha}_I(\lambda^*), \hat{\alpha}_R(\lambda^*))$.

We include three baselines: (i) Parametric quantile: $\hat{\lambda}$ is chosen as the 95%-quantile of $\|Y - \mu\|_\infty$, assuming $Y \sim \mathcal{N}(\hat{\mu}, \hat{\Sigma})$ with $\hat{\mu}$ and $\hat{\Sigma}$ estimated from the data. (ii) Empirical quantile: λ is taken as the 95% empirical quantile of $|y_i - \bar{y}|$. (iii) Conformal prediction: using $\mathbb{E}[Y]$ as the base predictor, we calibrate on Y to construct a 95%-valid ℓ_∞ -ball conformal set, and define $\hat{\lambda}$ as its radius [Patel et al., 2024b]. These baselines reflect the prevailing practice in robustness parameter selection, where the user would typically specify a small miscoverage level (*e.g.*, 5%) and then determine a data-driven $\hat{\lambda}$ that achieves the desired coverage.

Figure 4 presents the evaluation results. It can be seen that the estimated Pareto frontier (red) aligns closely with the true frontier (black), lying only slightly above it. This provides a clean visual supporting evidence to Figure 3 that our method is both valid and accurate. Furthermore, observe that in the newsvendor and portfolio selection problems, the ground-truth curves traced from varying λ contain points that are not strictly on the Pareto frontier (*i.e.*, non-dominant points), whereas the linear programming and shortest path problems yield well-defined Pareto frontiers. This observation is consistent with Assumption 3 and Proposition 3, where we argued that only some particular classes (*e.g.*, linear) are guaranteed to have full Pareto frontiers.

Next, observe from Figure 4 that the tradeoff points selected by the three baseline methods deviate substantially—achieving low miscoverage but suffering from high regret. In contrast, the point selected by CREME (red dot) lies very close to the true optimal trade-

off point (black star), striking a balanced compromise between miscoverage and regret. This improvement stems from two factors. First, unlike the baselines that are designed to conservatively control miscoverage and thus myopically select suboptimal robustness parameters, CREME explicitly accounts for both miscoverage and regret, enabling it to identify a globally balanced solution. Second, the high accuracy of our estimator (as previously discussed) allows CREME to closely trace the true Pareto frontier, thereby preserving the correct relative positioning of tradeoff points and guiding the selection of appropriate robustness parameters. Together, these results demonstrate that CREME effectively supports decision-makers in selecting robustness levels that achieve a desired balance between miscoverage and regret.

5 Conclusion

We proposed CREME, a conformalized framework for robust decision-making that certifies both miscoverage and regret across robustness levels, enabling practitioners to select appropriate robustness in optimization design. Theoretically, we showed that under mild conditions, the estimator provides conservative, distribution-free finite-sample guarantees and traces a certified Pareto frontier for the miscoverage–regret tradeoff. Empirically, across four canonical optimization paradigms, CREME produces frontiers with high validity and accuracy and guides robustness selection to balance miscoverage and regret. Thus, CREME offers a principled alternative to ad hoc calibration, addressing a key gap in the existing literature.

We note that while CREME itself is a lightweight procedure, its computational efficiency is ultimately bottlenecked by repeatedly solving the underlying optimization problem and its robust variant. Specifically, for each robustness level λ , the estimator requires solving up to $2n$ optimization problems, where n is the number of calibration samples. This cost can become substantial in high-dimensional or nonconvex settings. Nevertheless, in our experiments, spanning a wide range of convex optimization tasks, we find that CREME remains practical with standard solvers, and becomes particularly efficient when closed-form regret solutions are available. Looking ahead, we expect future work to focus on enhancing the scalability of CREME, thereby extending its applicability to more complex and large-scale decision problems.

References

[Agrawal et al., 2019] Agrawal, A., Amos, B., Barratt, S., Boyd, S., Diamond, S., and Kolter, Z. (2019). Differentiable convex optimization layers.

In *Advances in Neural Information Processing Systems*.

[Angelopoulos et al., 2022] Angelopoulos, A. N., Bates, S., Fisch, A., Lei, L., and Schuster, T. (2022). Conformal risk control. *arXiv preprint arXiv:2208.02814*.

[Balinsky and Balinsky, 2024] Balinsky, A. A. and Balinsky, A. D. (2024). Enhancing conformal prediction using e-test statistics. *arXiv preprint arXiv:2403.19082*.

[Ben-Tal and Nemirovski, 1999] Ben-Tal, A. and Nemirovski, A. (1999). Robust solutions of uncertain linear programs. *Operations research letters*, 25(1):1–13.

[Ben-Tal and Nemirovski, 2001] Ben-Tal, A. and Nemirovski, A. (2001). *Lectures on modern convex optimization: analysis, algorithms, and engineering applications*. SIAM.

[Ben-Tal and Nemirovski, 2002] Ben-Tal, A. and Nemirovski, A. (2002). Robust optimization—methodology and applications. *Mathematical programming*, 92(3):453–480.

[Bertsimas et al., 2011] Bertsimas, D., Brown, D. B., and Caramanis, C. (2011). Theory and applications of robust optimization. *SIAM review*, 53(3):464–501.

[Bertsimas and Kallus, 2020] Bertsimas, D. and Kallus, N. (2020). From predictive to prescriptive analytics. *Management Science*, 66(3):1025–1044.

[Bertsimas et al., 2012] Bertsimas, D., Litvinov, E., Sun, X. A., Zhao, J., and Zheng, T. (2012). Adaptive robust optimization for the security constrained unit commitment problem. *IEEE transactions on power systems*, 28(1):52–63.

[Beyer and Sendhoff, 2007] Beyer, H.-G. and Sendhoff, B. (2007). Robust optimization—a comprehensive survey. *Computer methods in applied mechanics and engineering*, 196(33–34):3190–3218.

[Chen et al., 2025] Chen, S., Zhu, S., and Sioshansi, R. (2025). Enhancing electricity-system resilience with adaptive robust optimization and conformal uncertainty characterization. *arXiv preprint arXiv:2505.11627*.

[Delage and Ye, 2010] Delage, E. and Ye, Y. (2010). Distributionally robust optimization under moment uncertainty with application to data-driven problems. *Operations research*, 58(3):595–612.

[Diamond and Boyd, 2016] Diamond, S. and Boyd, S. (2016). CVXPY: A Python-embedded modeling language for convex optimization. *Journal of Machine Learning Research*, 17(83):1–5.

[Fabozzi et al., 2007] Fabozzi, F. J., Kolm, P. N., Pachamanova, D. A., and Focardi, S. M. (2007). *Robust portfolio optimization and management*. John Wiley & Sons.

[Farinhas et al., 2023] Farinhas, A., Zerva, C., Ulmer, D., and Martins, A. F. (2023). Non-exchangeable conformal risk control. *arXiv preprint arXiv:2310.01262*.

[Gabrel et al., 2014] Gabrel, V., Murat, C., and Thiele, A. (2014). Recent advances in robust optimization: An overview. *European journal of operational research*, 235(3):471–483.

[Gauthier et al., 2025a] Gauthier, E., Bach, F., and Jordan, M. I. (2025a). Backward conformal prediction. *arXiv preprint arXiv:2505.13732*.

[Gauthier et al., 2025b] Gauthier, E., Bach, F., and Jordan, M. I. (2025b). E-values expand the scope of conformal prediction. *arXiv preprint arXiv:2503.13050*.

[Goldfarb and Iyengar, 2003] Goldfarb, D. and Iyengar, G. (2003). Robust portfolio selection problems. *Mathematics of operations research*, 28(1):1–38.

[Gunantara, 2018] Gunantara, N. (2018). A review of multi-objective optimization: Methods and its applications. *Cogent Engineering*, 5(1):1502242.

[Lam and Zhou, 2017] Lam, H. and Zhou, E. (2017). The empirical likelihood approach to quantifying uncertainty in sample average approximation. *Operations Research Letters*, 45(4):301–307.

[Lei et al., 2018] Lei, J., G’Sell, M., Rinaldo, A., Tibshirani, R. J., and Wasserman, L. (2018). Distribution-free predictive inference for regression. *Journal of the American Statistical Association*, 113(523):1094–1111.

[Lin et al., 2022] Lin, F., Fang, X., and Gao, Z. (2022). Distributionally robust optimization: A review on theory and applications. *Numerical Algebra, Control and Optimization*, 12(1):159–212.

[Mandi et al., 2024] Mandi, J., Kotary, J., Berden, S., Mulamba, M., Bucarey, V., Guns, T., and Fioretto, F. (2024). Decision-focused learning: Foundations, state of the art, benchmark and future opportunities. *Journal of Artificial Intelligence Research*, 80:1623–1701.

[Marler and Arora, 2004] Marler, R. T. and Arora, J. S. (2004). Survey of multi-objective optimization methods for engineering. *Structural and multidisciplinary optimization*, 26(6):369–395.

[Mohajerin Esfahani and Kuhn, 2018] Mohajerin Esfahani, P. and Kuhn, D. (2018). Data-driven distributionally robust optimization using the wasserstein metric: Performance guarantees and tractable reformulations. *Mathematical Programming*, 171(1):115–166.

[Papadopoulos et al., 2002] Papadopoulos, H., Proedrou, K., Vovk, V., and Gammerman, A. (2002). Inductive confidence machines for regression. In *Machine learning: ECML 2002: 13th European conference on machine learning Helsinki, Finland, August 19–23, 2002 proceedings 13*, pages 345–356. Springer.

[Patel et al., 2024a] Patel, Y., Rayan, S., and Tewari, A. (2024a). Conformal robust control of linear systems. *arXiv preprint arXiv:2405.16250*.

[Patel et al., 2024b] Patel, Y. P., Rayan, S., and Tewari, A. (2024b). Conformal contextual robust optimization. In *International Conference on Artificial Intelligence and Statistics*, pages 2485–2493. PMLR.

[Rahimian and Mehrotra, 2019] Rahimian, H. and Mehrotra, S. (2019). Distributionally robust optimization: A review. *arXiv preprint arXiv:1908.05659*.

[Teneggi et al., 2023] Teneggi, J., Tivnan, M., Stayman, W., and Sulam, J. (2023). How to trust your diffusion model: A convex optimization approach to conformal risk control. In *International Conference on Machine Learning*, pages 33940–33960. PMLR.

[Vovk et al., 2005] Vovk, V., Gammerman, A., and Shafer, G. (2005). *Algorithmic learning in a random world*, volume 29. Springer.

[Zhang et al., 2025] Zhang, J., Wang, F., Yu, P. S., Ding, K., and Zhu, S. (2025). Topology-aware conformal prediction for stream networks. *arXiv preprint arXiv:2503.04981*.

[Zhou et al., 2025] Zhou, W., Orfanoudaki, A., and Zhu, S. (2025). Conformalized decision risk assessment. *arXiv preprint arXiv:2505.13243*.

Supplementary Materials for “Conformalized Uncertainty Calibration for Balanced Decision Making”

A Illustrative Examples: When the Assumptions Hold (and When They Fail)

To better understand the scope and limitations of our assumptions, we provide two contrasting examples. The first demonstrates a setting in which all conditions are satisfied, showing that the proposition applies naturally in classical robust optimization problems. The second example highlights a case where the key *majorant consistency* assumption fails, which happens when actuation penalties are asymmetric or the predictive model is misspecified, illustrating the boundaries of our results and where caution is required in practice. Without loss of generality, we assume X to be degenerate in both examples, so that all arguments are marginalized with respect to Y .

Example (assumption holds) Consider a linear optimization with a compact convex feasible region

$$\min_z \langle Y, z \rangle \quad \text{s.t.} \quad \|z\|_2 \leq M,$$

and assume $\|Y\| \leq K$ a.s. (hence regret is uniformly bounded) and that measurable selectors are taken. We define nested uncertainty sets $\mathcal{C}_\lambda = \{y : \|y - \mu\|_2 \leq \lambda\}$, which by definition guarantees that the miscoverage is a decreasing function of λ . We define the robust variant of the optimization problem as

$$\min_z \max_{y \in \mathcal{C}_\lambda} \langle y, z \rangle \quad \text{s.t.} \quad \|z\|_2 \leq M.$$

Note that the inner maximization simplifies to the support function of the ball, *i.e.* $\langle \mu, z \rangle + \lambda \|z\|_2$, so plugging this result in and solving for the outer minimization problem gets

$$z_\lambda^* = \begin{cases} 0, & \lambda \geq \|\mu\|_2, \\ -M \cdot \mu / \|\mu\|_2, & \lambda < \|\mu\|_2. \end{cases}$$

Therefore, $\mathbb{E}[f(Y, z_\lambda^*)] = \langle \mu, z_\lambda^* \rangle \in \{0, -M\|\mu\|_2\}$ is weakly increasing as λ increasing, satisfying Assumption 3. Nesting holds by construction, and

$$R_\lambda(X, Y) = \langle Y, z_\lambda^* \rangle - \min_{\|z\|_2 \leq M} \langle Y, z \rangle \leq 2M\|Y\| \leq 2MK,$$

so $R_\lambda(X, Y) \leq B$ by setting $B = 2MK$, and it is easy to verify that $R_\lambda(X, Y) \leq B$ is an increasing function of λ , therefore the statements in Proposition 3 hold. In fact, the frontier in this example is *strictly decreasing* whenever $\mathbb{P}\{\|\mu\|_2 > \lambda\} > 0$ for some λ . This example illustrates that the assumption is mild and naturally satisfied in common robust linear programs with ellipsoidal uncertainty and bounded outcomes.

Remark 1. Note that this example naturally extends to the conditional setting, where μ is replaced by some estimator $\hat{g}(x)$ based on the covariate random variable X , and $\mathbb{E}[f(Y, z_\lambda^*)]$ is replaced by $\mathbb{E}[f(Y, z_\lambda^*) | X]$. All the arguments above remain true.

Counterexample (assumption fails) Let $Y \in \{-1, +1\}$ with $\mathbb{P}\{Y = +1\} = 0.9$, and decision variable space $\mathcal{Z} = [-1, 1]$. Define the objective function as

$$f(y, z) = \begin{cases} (z - y)^2 & \text{if } z \in [0, 1], \\ (z - y)^2 + \frac{1}{4} & \text{if } z \in [-1, 0]. \end{cases}$$

Define $\Lambda = \{\lambda_1, \lambda_2\}$ with $\lambda_1 < \lambda_2$, and nested uncertainty sets $\mathcal{C}_{\lambda_1} = \{-1\}$ and $\mathcal{C}_{\lambda_2} = \{-1, +1\}$. It can be seen that the (robust) solutions to $\min_z \max_{y \in \mathcal{C}_\lambda} f(y, z)$ can be divided into two cases: (i) When $\lambda = \lambda_1$, $z_{\lambda_1}^* = -1$; (ii) When $\lambda = \lambda_2$, $z_{\lambda_2}^* = 0$. Therefore, it can be seen that

$$\mathbb{E}[f(Y, z_{\lambda_1}^*)] = 0.9 \cdot (4 + 0.25) + 0.1 \cdot 0.25 = 3.85 > \mathbb{E}[f(Y, z_{\lambda_2}^*)] = 0.9 \cdot 1 + 0.1 \cdot 1 = 1,$$

which makes this optimization problem violate Assumption 3.

In the meantime, in this counterexample, while miscoverage is still a decreasing function of λ (from 0.9 under λ_1 to 0 under λ_2), the expected regret is no longer an increasing function of λ . Specifically, since $\min_{z \in [-1, 1]} f(+1, z) = 0$ (achieved at $z = 1$) and $\min_{z \in [-1, 1]} f(-1, z) = 0.25$ (achieved at $z = -1$), there is

$$\begin{aligned}\alpha_R(\lambda_1) &= \mathbb{E}[(4 + 0.25 - 0) \mathbb{1}\{Y = +1\} + (0.25 - 0.25) \mathbb{1}\{Y = -1\}] = 3.6 + 0.9 \cdot 0.25, \\ \alpha_R(\lambda_2) &= \mathbb{E}[(1 - 0) \mathbb{1}\{Y = +1\} + (1 - 0.25) \mathbb{1}\{Y = -1\}] = 0.9 + 0.1 \cdot (1 - 0.25),\end{aligned}$$

and hence $\alpha_R(\lambda_1) > \alpha_R(\lambda_2)$, making expected regret an decreasing function of λ .

In sum, in this example, all other conditions (nesting, measurability, bounded regret) hold, but the proposition fails without majorant consistency. This illustrates that asymmetric model/actuation costs or misspecified robust surrogates can break the decreasing trade-off.

B Proof for Proposition 2

Proof for Proposition 2. Notice the following decomposition:

$$|\hat{\alpha}_\ell(\lambda) - \mathbb{E}[\ell_\lambda(X_{n+1}, Y_{n+1})]| \leq |\hat{\alpha}_\ell(\lambda) - \tilde{\alpha}_\ell(\lambda)| + |\tilde{\alpha}_\ell(\lambda) - \mathbb{E}[\ell_\lambda(X_{n+1}, Y_{n+1})]|.$$

The first term can be upper-bounded by $1/(n+1)$ by the definition of $\hat{\alpha}_\ell(\lambda)$ and $\tilde{\alpha}_\ell(\lambda)$. The second term can be further expanded as

$$\begin{aligned}|\tilde{\alpha}_\ell(\lambda) - \mathbb{E}[\ell_\lambda(X_{n+1}, Y_{n+1})]| &= \left| \frac{n}{n+1} \bar{\ell}_n(\lambda) + \frac{B}{n+1} - \mathbb{E}[\ell_\lambda(X_{n+1}, Y_{n+1})] \right| \\ &= \left| \frac{n}{n+1} \{ \bar{\ell}_n(\lambda) - \mathbb{E}[\ell_\lambda(X_{n+1}, Y_{n+1})] \} + \frac{B}{n+1} - \frac{1}{n+1} \mathbb{E}[\ell_\lambda(X_{n+1}, Y_{n+1})] \right| \\ &\leq \frac{n}{n+1} |\bar{\ell}_n(\lambda) - \mathbb{E}[\ell_\lambda(X_{n+1}, Y_{n+1})]| + \frac{2B}{n+1},\end{aligned}$$

where for the last inequality we used the bounding condition (Assumption 2). Observe that by the *i.i.d.* condition, using Hoeffding's inequality, we know that for any $\delta > 0$, there is

$$|\bar{\ell}_n(\lambda) - \mathbb{E}[\ell_\lambda(X_{n+1}, Y_{n+1})]| \leq B \cdot \sqrt{\frac{1}{2n} \log\left(\frac{2}{\delta}\right)}, \quad w.p. \geq 1 - \delta.$$

Plugging this error term into the expansion above, we get

$$|\tilde{\alpha}_\ell(\lambda) - \mathbb{E}[\ell_\lambda(X_{n+1}, Y_{n+1})]| \leq \frac{nB}{n+1} \sqrt{\frac{1}{2n} \log\left(\frac{2}{\delta}\right)} + \frac{2B}{n+1} = \frac{B}{n+1} \left(\sqrt{\frac{n}{2} \log\left(\frac{2}{\delta}\right)} + 2 \right), \quad w.p. \geq 1 - \delta.$$

Therefore, plugging back into the original equation, we know that with probability no less than $1 - \delta$,

$$|\hat{\alpha}_\ell(\lambda) - \mathbb{E}[\ell_\lambda(X_{n+1}, Y_{n+1})]| \leq \frac{B}{n+1} \left(\sqrt{\frac{n}{2} \log\left(\frac{2}{\delta}\right)} + 2 \right) + \frac{1}{n+1} = \frac{B}{n+1} \left(\sqrt{\frac{n}{2} \log\left(\frac{2}{\delta}\right)} + 2 + \frac{1}{B} \right).$$

We've concluded the proof. \square

Using Proposition 2, we can further establish a reliable lower bound on the difference in the true expected loss function between two robustness parameters, as summarized below.

Corollary 2. *Given $\lambda_1, \lambda_2 \in \Lambda$ and $\lambda_1 \neq \lambda_2$, then with probability no less than $1 - \delta$, there is*

$$|\mathbb{E}[\ell_{\lambda_1}(X_{n+1}, Y_{n+1})] - \mathbb{E}[\ell_{\lambda_2}(X_{n+1}, Y_{n+1})]| \geq |\hat{\alpha}_\ell(\lambda_1) - \hat{\alpha}_\ell(\lambda_2)| - \frac{2B}{n+1} \left(\sqrt{\frac{n}{2} \log \left(\frac{1}{\delta} \right)} + 2 + \frac{1}{B} \right).$$

Proof of Corollary 2. Since for any $\lambda \in \Lambda$, we know from Proposition 2 that with probability $1 - \delta'$, there is

$$|\mathbb{E}[\ell_\lambda(X_{n+1}, Y_{n+1})] - \hat{\alpha}_\ell(\lambda)| \leq \frac{B}{n+1} \left(\sqrt{\frac{n}{2} \log \left(\frac{2}{\delta'} \right)} + 2 + \frac{1}{B} \right).$$

Therefore, by setting $\delta' = \delta/2$, we know that with probability at least $1 - \delta$, there is

$$\begin{aligned} & |\mathbb{E}[\ell_{\lambda_1}(X_{n+1}, Y_{n+1})] - \mathbb{E}[\ell_{\lambda_2}(X_{n+1}, Y_{n+1})] - (\hat{\alpha}_\ell(\lambda_1) - \hat{\alpha}_\ell(\lambda_2))| \\ & \leq |\mathbb{E}[\ell_{\lambda_1}(X_{n+1}, Y_{n+1})] - \hat{\alpha}_\ell(\lambda_1)| + |\mathbb{E}[\ell_{\lambda_2}(X_{n+1}, Y_{n+1})] - \hat{\alpha}_\ell(\lambda_2)| \\ & \leq \frac{2B}{n+1} \left(\sqrt{\frac{n}{2} \log \left(\frac{1}{\delta} \right)} + 2 + \frac{1}{B} \right). \end{aligned}$$

Rearranging, we get:

$$|\mathbb{E}[\ell_{\lambda_1}(X_{n+1}, Y_{n+1})] - \mathbb{E}[\ell_{\lambda_2}(X_{n+1}, Y_{n+1})]| \geq |\hat{\alpha}_\ell(\lambda_1) - \hat{\alpha}_\ell(\lambda_2)| - \frac{2B}{n+1} \left(\sqrt{\frac{n}{2} \log \left(\frac{1}{\delta} \right)} + 2 + \frac{1}{B} \right).$$

This finishes the proof. \square

The difference in the true expected loss function between two robustness parameters is particularly useful in practice, as it reflects how much gain or loss a decision-maker can expect when switching from λ_1 to λ_2 , as illustrated in Figure 1. Corollary 2 suggests that we can simply use the difference in estimators after offsetting with the error term 2ϵ to obtain a lower bound, which informs the decision maker of a conservative estimate of the change magnitude. Practically, this can help reliably assess the trade-offs involved in selecting different robustness levels, leading to more principled and robust decision-making.

C Proof for Certified Pareto Frontier

Proof for Proposition 3. By nesting, for any (X, Y) and $\lambda_1 \leq \lambda_2$, $\mathcal{C}_{\lambda_1}(X) \subseteq \mathcal{C}_{\lambda_2}(X)$, hence

$$\mathbb{1}\{Y \notin \mathcal{C}_{\lambda_1}(X)\} \geq \mathbb{1}\{Y \notin \mathcal{C}_{\lambda_2}(X)\}.$$

Taking expectations on both sides yields $\alpha_I(\lambda_1) \geq \alpha_I(\lambda_2)$.

Observe that

$$\alpha_R(\lambda) = \mathbb{E}[f(Y, z_\lambda^*(X))] - \mathbb{E}\left[\min_{z \in \mathcal{Z}} f(Y, z)\right].$$

The second term is independent of λ . By the law of iterated expectations and Assumption 3,

$$\mathbb{E}[f(Y, z_{\lambda_2}^*(X))] = \mathbb{E}[\mathbb{E}[f(Y, z_{\lambda_2}^*(X))|X]] \geq \mathbb{E}[\mathbb{E}[f(Y, z_{\lambda_1}^*(X))|X]] = \mathbb{E}[f(Y, z_{\lambda_1}^*(X))].$$

Therefore $\alpha_R(\lambda_1) \leq \alpha_R(\lambda_2)$.

Because as λ increases (*i.e.*, \mathcal{C}_λ expands), α_I weakly decreases while α_R weakly increases, the map $\lambda \mapsto (\alpha_I(\lambda), \alpha_R(\lambda))$ is (weakly) decreasing. Fix $\lambda \in \Lambda$. For any $\lambda' \neq \lambda$, if $\lambda' < \lambda$ then $\alpha_I(\lambda') \geq \alpha_I(\lambda)$ and $\alpha_R(\lambda') \leq \alpha_R(\lambda)$; if $\lambda' > \lambda$ the inequalities reverse. Hence no policy in the family $\{z_\lambda^*\}$ strictly improves both coordinates over z_λ^* . Therefore every image point is Pareto efficient, and the image is exactly the Pareto frontier achievable by this policy family. (Ties may occur if the inequalities become equalities for some $\lambda_1 < \lambda_2$). \square

Proof for Corollary 1. For a given λ , the coordinatewise inequalities imply $(\alpha_I(\lambda), \alpha_R(\lambda)) \preceq (\hat{\alpha}_I(\lambda), \hat{\alpha}_R(\lambda))$ in the product order on \mathbb{R}^2 . Hence $\hat{\mathcal{S}}$ is an outer (safe) approximation of the true risk set $\mathcal{S} := \{(\alpha_I(\lambda), \alpha_R(\lambda)) : \lambda \in \Lambda\}$. Taking the set of non-dominated points (lower-left envelope) of $\hat{\mathcal{S}}$ yields certified trade-offs: any selected λ on this envelope admits guarantees $\mathbb{E}[I_\lambda(X, Y)] \leq \hat{\alpha}_I(\lambda)$ and $\mathbb{E}[R_\lambda(X, Y)] \leq \hat{\alpha}_R(\lambda)$ (by the direction of the bounds), *i.e.*, a certified Pareto frontier. \square

D Additional Experiment Details

Similar to Section A, the synthetic data used in our experiments focuses on settings where X is degenerated, so we only have observations of Y . As we've mentioned before, this simplification does not limit the generality of our experimental findings, since both the Pareto frontier and its associated performance metrics are inherently unconditioned on X . The implementation is developed in Python, with core dependencies on the `cvxpy` [Diamond and Boyd, 2016] and `cvxpylayers` [Agrawal et al., 2019] libraries, which are used to solve convex optimization problems. We use the default parameter settings in their libraries across all experiments. Across all settings, the upper bound B is heuristically set to the maximum observed regret for a large number (1×10^2) of simulations.

D.1 Experimental Setups

In this section, we present the detailed experimental setups for the four optimization problems considered in our study. Across all settings, we specify the uncertainty set as $\mathcal{C}_\lambda = \{\tilde{y} : \|\tilde{y} - \mu\|_\infty \leq \lambda\}$, where μ denotes the mean of the distribution of the outcome variable Y . These optimizations are solved via convex solvers in our implementation.

Linear Programming We consider a two-dimensional linear programming (LP), defined as

$$\min_{z \in \mathbb{R}^2} Y^\top z \quad \text{s.t.} \quad Az \leq b,$$

where Y is a bivariate uniform random variable supported on $[-2.1, -0.1] \times [-2, 0]$. We specify the feasible region as a triacontagon (*a.k.a.* 32-gon) centered at the origin, intersecting the positive orthant. Specifically, the parameters $A \in \mathbb{R}^{34 \times 2}$ and $b \in \mathbb{R}^{34}$ are defined as:

$$A_i = \left(\cos\left(\frac{2\pi}{32} \times i\right), \sin\left(\frac{2\pi}{32} \times i\right) \right), \quad b_i = (1, 1), \quad \forall i = 1, \dots, 32.$$

and the last two rows of A and b are configured to ensure the positivity of z on both dimensions. The robust variant of this problem is defined as

$$\min_{z \in \mathbb{R}^2} \max_{y \in \mathcal{C}_\lambda} y^\top z \quad \text{s.t.} \quad Az \leq b.$$

This robust optimization problem can be equivalently reformulated as another LP

$$\min_{z, t \in \mathbb{R}^2} \mu^\top z + \lambda \mathbf{1}^\top t \quad \text{s.t.} \quad Az \leq b, \quad -t \leq z \leq t, \quad t \geq 0,$$

where $\mathbf{1} = [1, 1]^\top$ is an all-ones vector and t serves as an auxiliary variable to linearize the ℓ_∞ -norm.

Newsvendor We consider a standard single-item inventory (newsvendor) problem, defined as

$$\min_{z \in \mathbb{R}_+} [-p \min(Y, z) + cz - v(z - Y)^+],$$

where z denotes the stocking quantity Y the random demand, p the unit selling price, c the unit procurement cost, and v the unit salvage value for unsold inventory. This objective captures the trade-off between the profit from meeting demand and the loss due to overstocking or understocking. We simulate demands Y as a univariate uniform random variable supported on $[1, 3]$, and the parameters are set to $(p, c, v) = (3, 2, 0)$. The robust variant of the newsvendor problem is defined as

$$\min_{z \in \mathbb{R}_+} \max_{y \in \mathcal{C}_\lambda} [-p \min(y, z) + cz - v(z - y)^+].$$

Since both the original problem and the robust problem admit closed-form solutions, we can plug the solutions into the regret expression to get:

$$R_\lambda(X, Y) = p(Y - \min\{Y, \mu - \lambda\}) - c(Y - (\mu - \lambda)).$$

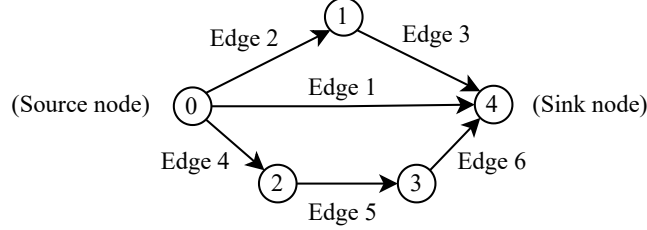


Figure 5: An example illustration of a network with three paths considered in our shortest path optimization.

Portfolio Selection We study a long-only portfolio selection problem with CVaR regularization. Let $Y \in \mathbb{R}^2$ denote the return scenario for two assets, which is specified as a bivariate uniform random variable supported on $[1, 3] \times [1, 3]$. Let $z \in \mathbb{R}^2$ be the decision variable. For a given confidence level $\alpha \in (0, 1)$ and some risk-aversion parameter $\gamma > 0$, the optimization problem is defined as

$$\min_{z \in \mathbb{R}^2} -Y^\top z - \gamma \text{CVaR}_\alpha(Y^\top z),$$

where the parameters are specified as $(\gamma, \alpha) = (1, 0.95)$. This problem can be reformulated into an explicit convex optimization by introducing an auxiliary VaR variable $t \in \mathbb{R}$ and slack variables $u_i \in \mathbb{R}$:

$$\min_{z, t, u} -Y^\top z + \gamma \left(t + \frac{1}{(1-\alpha)n} \sum_{i=1}^n u_i \right) \quad \text{s.t.} \quad \mathbf{1}^\top z = 1, \quad z \geq 0, \quad u_i \geq -y_i^\top z - t, \quad u_i \geq 0.$$

Here, y_i denotes a separate set of realized set of return scenarios for computing the empirical CVaR. The robust optimization variant can be reformulated by adding an ℓ_1 penalty on z and replaces Y by μ to the original optimization problem:

$$\min_{z, t, u} -\mu^\top z + \gamma \left(t + \frac{1}{(1-\alpha)n} \sum_{i=1}^n u_i \right) + \lambda \|z\|_1 \quad \text{s.t.} \quad \mathbf{1}^\top z = 1, \quad z \geq 0, \quad u_i \geq -y_i^\top z - t, \quad u_i \geq 0.$$

Shortest Path The shortest path problem is formulated on a directed acyclic network with multiple parallel source–sink paths of varying lengths, as illustrated in Figure 5. The objective is to find the least-cost flow that satisfies flow conservation while minimizing travel cost under uncertainty.

Let the network be represented by its node–edge incidence matrix $A \in \mathbb{R}^{n \times m}$ and a supply–demand vector for each node $b \in \mathbb{R}^n$, where $b_0 = 1$ and $b_n = -1$ denote the source and sink nodes, respectively. The decision variable $z \in \mathbb{R}_+^m$ encodes the flow through each edge, and the Gaussian random vector $Y \in \mathbb{R}^m$ specifies the cost on each edge. The nominal (stochastic) shortest path problem is then

$$\min_{z \in \mathbb{R}_+^m} Y^\top z \quad \text{s.t.} \quad Az = b.$$

Since the shortest-path problem is linear, its robust counterpart—and its equivalent convex reformulation—can be written as

$$\min_{z \in \mathbb{R}_+^m} \max_{y \in \mathcal{C}_\lambda} y^\top z \quad \text{s.t.} \quad Az = b. \iff \min_{z \in \mathbb{R}_+^{n_{\text{edge}}}} \mu^\top z + \lambda (w^\top z) \quad \text{s.t.} \quad Az = b,$$

where $w \in \mathbb{R}_+^{n_{\text{edge}}}$ is a vector of per-edge sensitivity coefficients. Namely, robustness inflates the nominal cost by a weighted ℓ_1 penalty on flow magnitude.

In our implementation, we specify the network to have five paths, with a gradually decreasing mean of the length random variable Y . Please refer to our source code for more detailed specifications.

D.2 Additional Experiment Results

In this section, we provide additional experimental details and results that were omitted from the main paper.

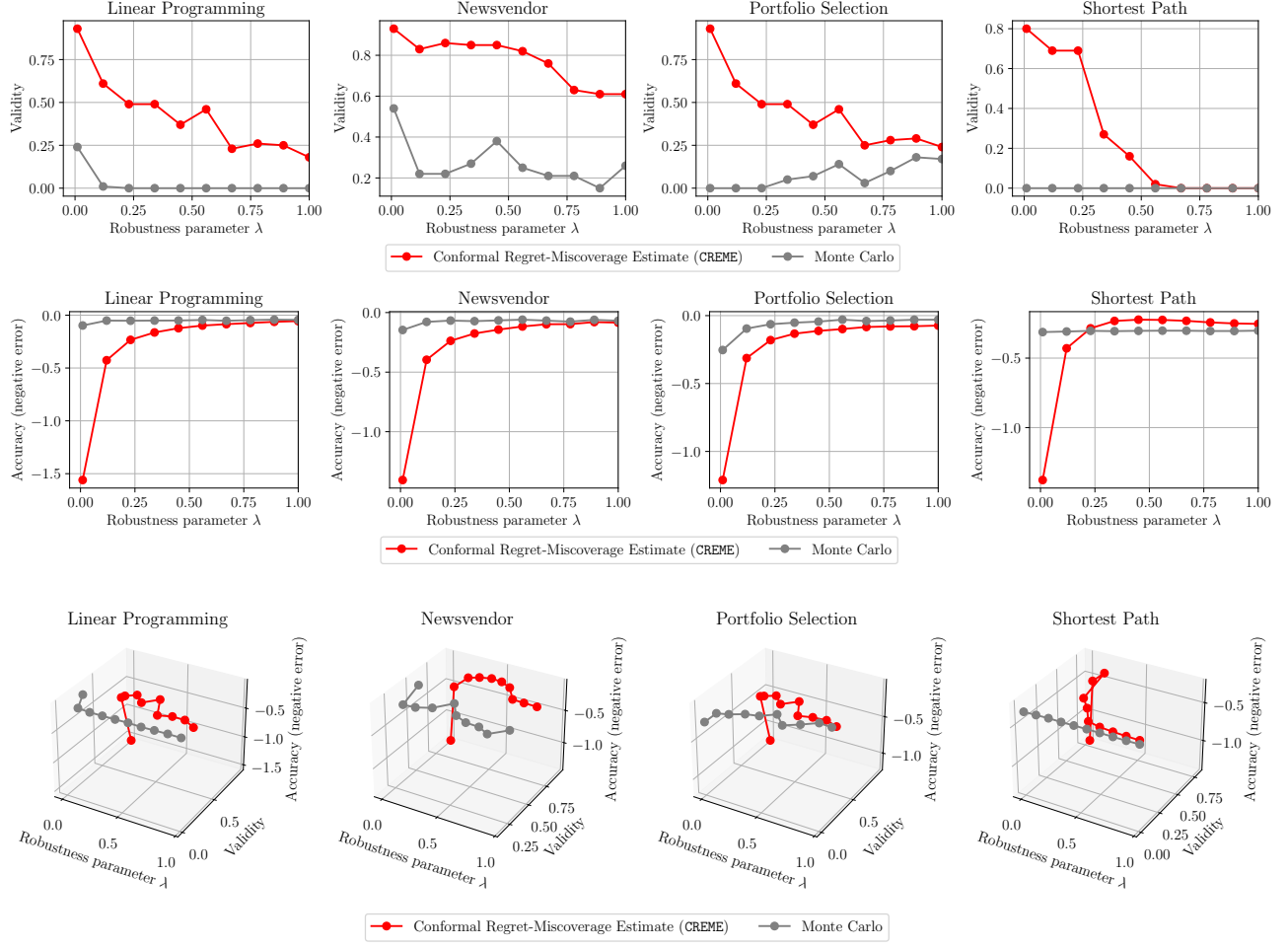


Figure 6: Validity-accuracy tradeoff curves under four optimization settings. *First row*: validity versus robustness parameter λ . *Second row*: accuracy versus robustness parameter λ . *Third row*: a 3D view of the two metrics and the robustness parameter λ .

D.3 Detailed Setups

Validity-Accuracy Analysis We provide additional mathematical details of the evaluation metrics used in the validity-accuracy analysis experiment. Let the number of trials be $T = 20$. For each prespecified robustness parameter $\lambda \in \Lambda$, the validity and accuracy metrics are defined as:

$$\text{Validity} = \frac{1}{T} \sum_{t=1}^T \mathbb{1}\{\hat{\alpha}_R(\lambda) \geq \alpha_R(\lambda)\} \cdot \mathbb{1}\{\hat{\alpha}_I(\lambda) \geq \alpha_I(\lambda)\}.$$

$$\text{Accuracy} = -\frac{1}{T} \sum_{t=1}^T \sqrt{(\hat{\alpha}_R(\lambda) - \alpha_R(\lambda))^2 + (\hat{\alpha}_I(\lambda) - \alpha_I(\lambda))^2}.$$

In our implementation, these metrics are further averaged over all $\lambda \in \Lambda$, where Λ is chosen such that the corresponding uncertainty sets achieve miscoverage rates ranging from 0% to 100%. This range is determined by the radius of the support of the distribution of the random outcome Y . Finally, the estimators $\hat{\alpha}_\ell(\lambda)$ are computed by averaging over 10 independent replications to obtain smoother estimates.

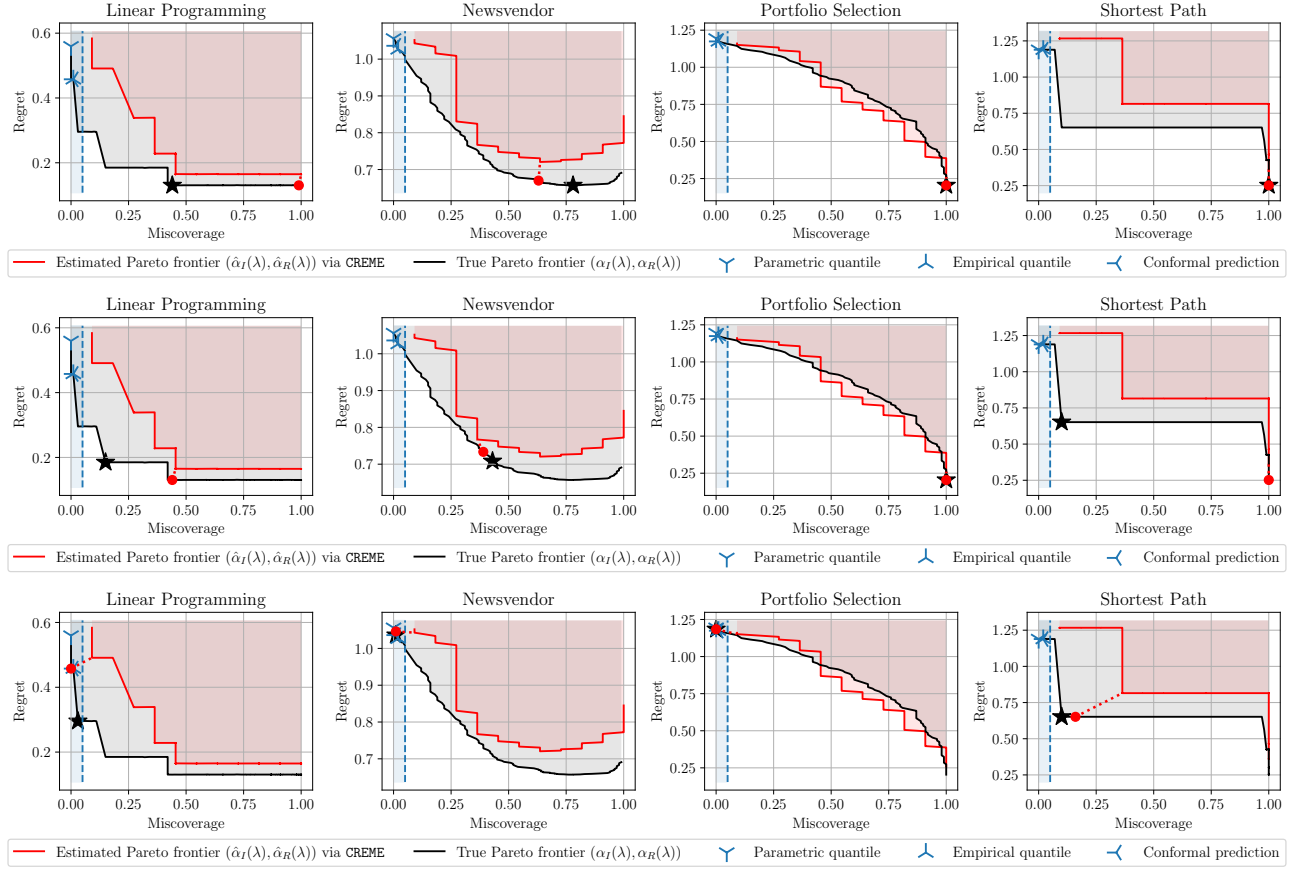


Figure 7: Miscoverage-regret tradeoff Pareto frontiers with attained solutions from each model under different preference weights. *First row*: tradeoff points identified using weight $w_1 = 0, w_2 = 1$. *Second row*: tradeoff points identified using weight $w_1 = \sqrt{2}/2, w_2 = \sqrt{2}/2$. *Third row*: tradeoff points identified using weight $w_1 = 1, w_2 = 0$.

Decision Quality Evaluation We provide additional details for the setup of the decision quality evaluation experiment. When constructing the certified Pareto frontier estimated from CREME as well as for the baseline methods in estimating $\hat{\lambda}$, we use a total of $n = 10$ calibration data. The optimal solution of the tradeoff is the plug-in of the estimated optimal robustness parameter $\hat{\lambda}$. The estimated tradeoff point from CREME is defined as $\hat{\lambda} = \min_{\lambda} [w_1 \cdot \hat{\alpha}_I(\lambda) + w_2 \cdot \hat{\alpha}_R(\lambda)]$. Similarly, the optimal tradeoff point from the true Pareto frontier is defined as $\lambda^* = \min_{\lambda} [w_1 \cdot \alpha_I(\lambda) + w_2 \cdot \alpha_R(\lambda)]$.

D.4 Additional Results

Figure 6 provides a detailed breakdown of the validity-accuracy performance evaluation originally presented in Figure 3 of the main paper. Consistent with the observations discussed in the main text, it is now more clearly visible that as the robustness parameter λ (*i.e.*, the radius of the uncertainty set) increases, the validity of CREME decreases approximately linearly, whereas its accuracy improves at an almost exponential rate. These results further substantiate our earlier claim regarding the superior performance of CREME over the naive Monte Carlo estimator.

Figure 7 parallels Figure 4 in the main paper, but presents additional trade-off points attained by different methods under varying specifications of the preference weightings. It can be observed that across different weight configurations, the three baseline methods (parametric quantile, empirical quantile, and conformal prediction) perform well only in the last row, which corresponds to a weighting of $w_1 = 1, w_2 = 0$. This behavior is expected, as this particular weighting places greater emphasis on minimizing miscoverage, which is the primary objective of these baselines. In contrast, CREME consistently identifies near-optimal solutions that lie close to the true

Pareto-optimal trade-off points across all weighting specifications. These results further support our main claim that CREME serves as a principled and flexible framework for identifying optimal trade-offs between regret and miscovariance under diverse decision-maker preferences.